Contribution from the Department of Chemical and Biological Sciences, Oregon Graduate Center, Beaverton, Oregon 97006-1999

One-Electron Reduction of Dihexadecyl Phosphate Vesicle Bound Viologens by Pentacyanocobaltate(II) Ion

James K. Hurst* and David H. P. Thompson

Received July 25, 1986

N-Methyl-*N'*-alkyl-4,4'-bipyridinium (C_nMV^{2+}) ions bound to dihexadecyl phosphate (DHP) vesicles are rapidly reduced to radical cations by $Co(CN)_5^{3-}$ in alkaline solutions containing cyanide ion. For the short-chain viologens investigated ($n \leq 10$), the predominant pathway obeys the rate law $d[C_nMV^+]/dt = a[C_nMV^{2+}]/(b + c[C_nMV^{2+}])$, where a is pseudo first order in $[Co(CN)_5^{3-}]$ and $[CN^-]$ under the experimental conditions. Reaction rates for longer chain viologens ($n \geq 14$) are several-fold slower at comparable reactant concentrations; the kinetic traces are biphasic, with both components first order in $[C_nMV^{2+}]$ and pseudo first order in $[Co(CN)_5^{3-}]$ and $[CN^-]$. A mechanism consistent with the data comprises outer-sphere electron transfer preceded by $Co(CN)_5^{3-}$ ligation of a sixth CN^- ion. This mechanism was confirmed for C_6MV^{2+}–DHP vesicles by quantitative isolation and spectrophotometric identification of $Co(CN)_6^{3-}$ ion as the Co(III) product. The biphasic reduction of the long-chain viologens was taken as evidence for two distinct binding environments within DHP vesicles. The significance of these findings is discussed within the context of other studies on the dynamic properties of C_nMV^{2+}–DHP particles.

Introduction

The dynamics of chemical reactions can be profoundly altered by interfacial adsorption of one or both reactants. In addition to the general effects of microphase compartmentation and reduction of spatial dimensionality,[1] kinetic complexity can be introduced from the simultaneous existence of multiple binding domains,[2,3] reactant surface aggregation and lateral phase separation,[4] and, for bilayer membranes, differing reactivities of components located on the opposite surfaces to a reactant added asymmetrically, i.e., to just the external aqueous phases.[5] As part of a program investigating mechanisms of transmembrane redox in vesicles,[6-8] we have sought to characterize by kinetic analysis the nature of binding of *N*-methyl-*N'*-alkyl-4,4'-bipyridinium (C_nMV^{2+}) ions to anionic dihexadecyl phosphate (DHP) vesicles.[8,9] We report herein the kinetics of one-electron reduction of DHP-bound C_nMV^{2+} ions by pentacyanocobaltate(II) ion. A unique feature of this reaction is that the rate-limiting step changes with variation in the alkyl chain length. This effect is manifested only because the anionic vesicle surface exerts a strongly repulsive electrostatic force on the reductant. Other aspects of these reactions are compared to those with other chemical and photochemical reductants; the combined results give a self-consistent picture in which the shorter chain viologen analogues ($n \leq 10$) are only surface bound to the vesicle but the longer chain analogues exist simultaneously in both surface-bound and intercalated states.

Experimental Section

Reagents. *N*-Methyl-*N'*-alkyl-4,4'-bipyridinium chloride salts were synthesized and characterized as previously discussed.[8,9] Dihexadecyl phosphate vesicles were prepared by ultrasonic dispersal using the general procedures described previously[8,9] and were loaded with C_nMV^{2+} ions by adding stock viologen solutions while stirring rapidly. Suspensions were clarified by ultracentrifugation at 100000*g* and the analytical concentrations of C_nMV^{2+} ions determined by ultraviolet spectroscopy[8] using vesicles containing no viologen as reference to correct for background scatter. When prepared in this fashion, the suspensions contain a unimodal population of spherical unilamellar vesicles with a relatively narrow size distribution, as determined by quasi-elastic light scattering,[10] having mean particle hydrodynamic radii of ~160 Å and aggregate numbers of $\sim 1.5 \times 10^4$ DHP monomers. Pentacyanocobaltate(II) ion was prepared by mixing anaerobic solutions containing cobaltous nitrate and potassium cyanide; because $Co(CN)_5^{3-}$ ion undergoes slow decomposition,[11] it was formed directly in the reservoir of a stopped-flow apparatus and used immediately in the kinetic runs. Cobaltous ion concentrations of reagent stock solutions were determined by analysis[12] as $Co(SCN)_4^{2-}$; CN^- ion was determined by complexometric titration[13] in aqueous ammonia with $AgNO_3$.

All reactant solutions were adjusted to pH 11.4 with NaOH; when necessary, KNO_3 was added to maintain an ionic strength of $\mu = 0.05$ M. Nitrate was chosen as the counterion because it is chemically "innocent" and, being also innocuous in the Hofmeister series,[14] should tend not to destabilize the vesicles. Qualitatively, this latter expectation was realized. Both ClO_4^- and trifluoroacetate ion, which are high in the Hofmeister series, prevented vesicle formation when present in suspensions at concentration levels above 0.1 M, but vesicles formed readily at comparable levels of NO_3^- or Cl^- ion. Reagent solutions were purged of oxygen by bubbling with argon for ~1 h. Loss of cyanide as HCN during outgassing was shown to be negligible by Liebig titration; for instance, ~5% of the cyanide was lost from a 1.0 M KCN solution (pH 11) after 4 h of vigorous bubbling.

All reagent solutions were prepared from water that had been purified by reverse-osmosis ion exchange, followed by distillation in a quartz still. Unless otherwise specified, chemicals were the best available commercial materials.

Kinetic Instrumentation and Analyses. Stopped-flow kinetic measurements were made on Gibson-type instrument[15] fitted with anaerobic reactant solution reservoirs. The drive syringes were Hamilton gastight with Teflon plunger tips, and all connecting lines between reservoirs, drive syringes, and mixing block were enclosed within thick-walled Tygon tubing through which argon continuously flowed. This arrangement minimized introduction of adventitious oxygen during the runs. Transient voltage–time waveforms were captured on a Nicolet 4094A/4562 digital oscilloscope interfaced to a DEC Pro-350 computer. Reactions were monitored by following the appearance of the C_nMV^+ radical cations, generally at 605 nm. Depending upon reactants and medium conditions, the waveforms exhibited behavior that was either biphasic first order or

(1) Rothenberger, G.; Moser, J.; Grätzel, M.; Serpone, N.; Sharma, D. K. *J. Am. Chem. Soc.* **1985**, *107*, 8054–8059. Hatlee, M. D.; Kozak, J. J.; Rothenberger, G.; Infelta, P. P.; Grätzel, M. *J. Phys. Chem.* **1980**, *84*, 1508–1519. Fendler, J. H. *Annu. Rev. Phys. Chem.* **1984**, *35*, 137–157.
(2) Suddaby, B. R.; Brown, P. E.; Russell, J. C.; Whitten, D. G. *J. Am. Chem. Soc.* **1985**, *107*, 5609–5617.
(3) Schanze, K. S.; Shin, D. M.; Whitten, D. G. *J. Am. Chem. Soc.* **1985**, *107*, 507–509. Mizutani, T.; Whitten, D. G. *J. Am. Chem. Soc.* **1985**, *107*, 3621–3625. Ishiwara, T.; Fendler, J. H. *J. Am. Chem. Soc.* **1984**, *106*, 1908–1912. Ford, W. E.; Tollin, G. *Photochem. Photobiol.* **1983**, *38*, 441–449. Moss, R. A.; Schreck, R. P. *J. Am. Chem. Soc.* **1983**, *105*, 6767–6768. Almgren, M. *J. Phys. Chem.* **1981**, *85*, 3599–3603.
(4) Kunitake, T.; Ihara, H.; Okahata, Y. *J. Am. Chem. Soc.* **1983**, *105*, 6070–6078. Nakashima, N.; Morimitsu, K.; Kunitake, T. *Bull. Chem. Soc. Jpn.* **1984**, *57*, 3253–3257. Cellarius, R. A.; Mauzerall, D. *Biochim. Biophys. Acta* **1966**, *112*, 235–255.
(5) Moss, R. A.; Bizzigotti, G. O. *J. Am. Chem. Soc.* **1981**, *103*, 6512–6514. Moss, R. A.; Ihara, Y.; Bizzigotti, G. O. *J. Am. Chem. Soc.* **1982**, *104*, 7476–7478.
(6) Hurst, J. K.; Thompson, D. H. P. *J. Membr. Sci.* **1986**, *28*, 3–29. Lee, L. Y. C.; Hurst, J. K. *J. Am. Chem. Soc.* **1984**, *106*, 7411–7418.
(7) Hurst, J. K.; Lee, L. Y. C.; Grätzel, M. *J. Am. Chem. Soc.* **1983**, *105*, 7048–7056.
(8) Thompson, D. H. P.; Barrette, W. C., Jr.; Hurst, J. K. *J. Am. Chem. Soc.*, in press.
(9) Hurst, J. K.; Thompson, D. H. P.; Connolly, J. S. *J. Am. Chem. Soc.*, in press.
(10) Humphry-Baker, R.; Hurst, J. K.; Thompson, D. H. P., manuscript submitted for publication.
(11) King, N. K.; Winfield, M. E. *J. Am. Chem. Soc.* **1961**, *83*, 3366–3373.
(12) Kitson, R. E. *Anal. Chem.* **1950**, *22*, 664–667.
(13) See, e.g.: Kolthoff, I. M.; Sandell, E. B. *Textbook of Quantitative Inorganic Analysis*, 3rd ed.; Macmillan: New York, 1952; pp 458–460, 546–547.
(14) See, e.g.: Jencks, W. P. *Catalysis in Chemistry and Enzymology*; McGraw-Hill: New York, 1969; pp 358–360.
(15) Norton, K. A., Jr.; Hurst, J. K. *J. Am. Chem. Soc.* **1978**, *100*, 7237–7242.

0020-1669/87/1326-0039$01.50/0

mixed zero and first order in $[C_nMV^{2+}]$, the limiting reagent. The biphasic experimental curves were analyzed as concurrent first-order processes following conventional procedures. The mixed-order reactions were fitted to the equation

$$d[C_nMV^+]/dt = a[C_nMV^{2+}]/(b + c[C_nMV^{2+}]) \quad (1)$$

by determining directly the rates of reaction at various $[C_nMV^{2+}]$ values from tangents drawn to curves in plots of $[C_nMV^{2+}]$ vs. time; $[C_nMV^{2+}]$ values were determined from the waveforms at various times from the relation $[C_nMV^{2+}] = \Delta Abs/\epsilon(C_nMV^+)$, where the molar extinction coefficient[16] for the radical cation at 605 nm was taken to be $\epsilon(C_nMV^+) = 1.4 \times 10^4\ M^{-1}\ cm^{-1}$. Since $(d[C_nMV^+]/dt)^{-1} = b/a[C_nMV^{2+}]^{-1} + c/a$, the kinetic constants b/a and c/a can be evaluated from the slope and intercept, respectively, of the reciprocal plot.

Optical spectra were recorded on a Perkin-Elmer Lambda 9 instrument.

Results

Reaction Products and Stoichiometries. All of the viologens used in these studies adsorb strongly onto DHP vesicles, as is evident from their ultrafiltration and chromatographic behavior on dextran gels and strong-acid cation-exchange resins.[7] In the experiments described, the C_nMV^{2+}/DHP ratios were kept low, i.e., 1/200–1/400; under these conditions, the product DHP-bound viologen radical cations were monomeric, i.e., did not aggregate, as was indicated by their visible absorption band shapes.[17] The reduction of DHP-bound C_6MV^{2+} and $C_{16}MV^{2+}$ ions was examined quantitatively with use of a special 1-cm optical cuvette fitted with a double-septum antechamber to minimize introduction of adventitious oxygen during syringe transfer of reductant. On the basis of previously determined molar extinction coefficients for DHP-bound C_nMV^{2+} ion[9] and with the assumption of a value for C_nMV^+–DHP identical with that for the methylviologen radical cation,[16] the results obtained by reduction with excess $Co(CN)_5^{3-}$ ion are $C_6MV^+/C_6MV^{2+} = 1.1_3$ and $C_{16}MV^+/C_{16}MV^{2+} = 1.0_7$, indicating that all of the DHP-bound viologen is accessible to the reductant and that the reaction is driven to completion under the conditions of the kinetic analyses. The stoichiometric ratio exceeds the theoretical limit by about 10%, which is probably a consequence of our inability to correct exactly for the fairly strong UV background scattering by DHP vesicles. Typically, we observe slightly greater scatter from vesicles that do not contain viologen, which would lead to underestimation of the C_nMV^{2+} concentration.

The cobalt reaction product was identified by reacting $Co(CN)_5^{3-}$ ion with DHP-bound C_6MV^{2+} ion in slight excess. The reaction was carried out in 0.05 M KCN (pH 11.1) with 0.07 mM $Co(CN)_5^{3-}$ ion and 0.08 mM C_6MV^{2+} bound to 2 mM DHP, $[C_6MV^{2+}]/[DHP] = 1/25$. Under these conditions, the viologen radical formed is a mixture of monomeric and multimeric forms.[17] Following the reaction, the product solution was oxygenated, acidified with HCl to precipitate the vesicles, outgassed with N_2 to remove HCN, and passed down a Dowex 50 cation-exchange column to remove C_6MV^{2+} ion. The eluate following the void volume was analyzed spectrophotometrically. A single weakly absorbing peak was observed in the near-UV region at 305 nm with a second UV band at ~260 nm appearing as a shoulder on intense UV absorption at shorter wavelengths. A second experiment was carried out with methylviologen in the absence of vesicles where higher concentrations of reactants could be used. By the same procedures with 2.0 mM $Co(CN)_5^{3-}$ and 4.5 mM MV^{2+} ion as reactants, the optical spectrum of the cobalt product containing solution comprised two ultraviolet peaks located at 310 and 257 nm with an intensity ratio $I_{310}/I_{257} = 1.3$. This spectrum is nearly identical with that reported for $Co(CN)_6^{3-}$ ion;[18] quantitatively, the product yield calculated from $\epsilon_{310} = 191$ gives $[Co(CN)_6^{3-}] = 2.0$ mM, indicating stoichiometric conversion to the hexacyanocobaltate(III) ion. For reaction with C_6MV^{2+}–DHP, similar calculations indicate a $Co(CN)_6^{3-}$ yield of 1.4,

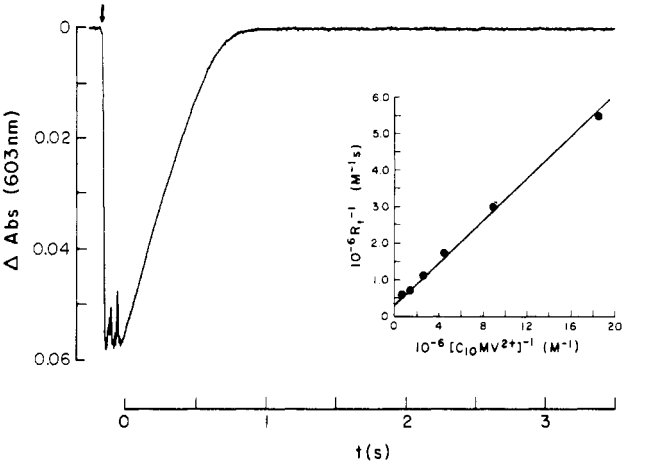

Figure 1. Kinetic trace of $C_{10}MV^{2+}$–DHP reduction by $Co(CN)_5^{3-}$ ion. Conditions: 5.0 μM $C_{10}MV^{2+}$, 0.3 mM $Co(CN)_5^{3-}$, 2 mM DHP in 0.05 M KCN, pH 11.4, 23 °C. The arrow shows onset of flow in the stopped-flow spectrophotometer; $t = 0$ corresponds to the point at which flow ceased. Inset: reciprocal of rates (R_i) plotted as the inverse of reactant alkylviologen concentration according to eq 1. The line is the least-squares fit to the data points.

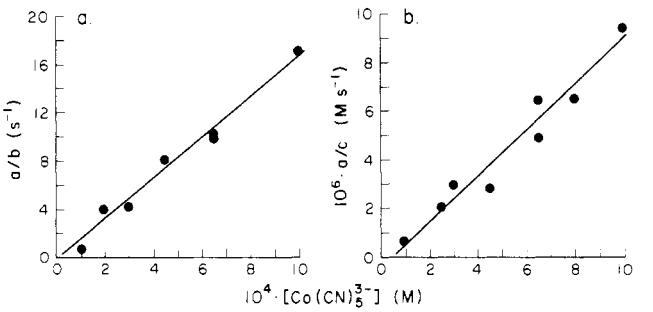

Figure 2. $Co(CN)_5^{3-}$ ion dependences of rate parameters for $C_{10}MV^{2+}$–DHP reduction: (a) first-order term according to eq 1; (b) zero-order term. Conditions: 0.05 M KCN, 2 mM DHP, 4.7–6.1 μM $C_{10}MV^{2+}$, pH 11.4, 23 °C. Data points are averages of four individual runs; lines are least-squares fits to the points.

although tailing of a UV-absorbing impurity makes quantitative assessment difficult. In any event, the absence of detectable bands at longer wavelengths excludes other commonly found oxidized cobalt species,[18,19] notably $Co(CN)_5OH_2^{2-}$, $[Co(CN)_5]_2O_2^{6-}$, and $[Co(CN)_5]_2O_2^{5-}$ ions. The reactions under study therefore correspond to the equation

$$CN^- + Co(CN)_5^{3-} + C_nMV^{2+}\text{–DHP} \rightarrow Co(CN)_6^{3-} + C_nMV^+\text{–DHP} \quad (2)$$

Kinetics. For reactions with the short-chain viologens ($n \leq 10$), radical cation formation followed mixed zero- and first-order kinetics under the experimental conditions. The zero-order component was most evident for $C_{10}MV^{2+}$–DHP particles (Figure 1); the inset shows the data treated according to eq 1, which adequately accounts for the dynamic behavior of this system. Both slopes and intercepts of these plots were inversely dependent upon CN^- and $Co(CN)_5^{3-}$ concentration levels, i.e., $a/b = k[Co(CN)_5^{3-}][CN^-]$ and $a/c = k'[Co(CN)_5^{3-}][CN^-]$. The $Co(CN)_5^{3-}$ ion dependence for both terms is given for $C_{10}MV^{2+}$–DHP in Figure 2.

For C_6MV^{2+} and, to a lesser extent, C_8MV^{2+}, the zero-order character is less prominent at the lowest $Co(CN)_5^{3-}$ and CN^- concentration levels investigated. This suggests an additional kinetic term in the rate law that is independent of the product $[Co(CN)_5^{3-}][CN^-]$. However, its functional dependence could not be determined because it made only minor contribution to the overall reaction under most experimentally accessible conditions.

(16) Watanabe, T.; Honda, K. *J. Phys. Chem.* **1982**, *86*, 2617–2619.
(17) Meisel, D.; Mulac, W. A.; Matheson, M. S. *J. Phys. Chem.* **1981**, *85*, 179–189.
(18) Bayston, J. H.; Beale, R. N.; King, N. K.; Winfield, M. E. *Aust. J. Chem.* **1963**, *16*, 954–968.
(19) Birk, J. P.; Halpern, J. *J. Am. Chem. Soc.* **1968**, *90*, 305–309.

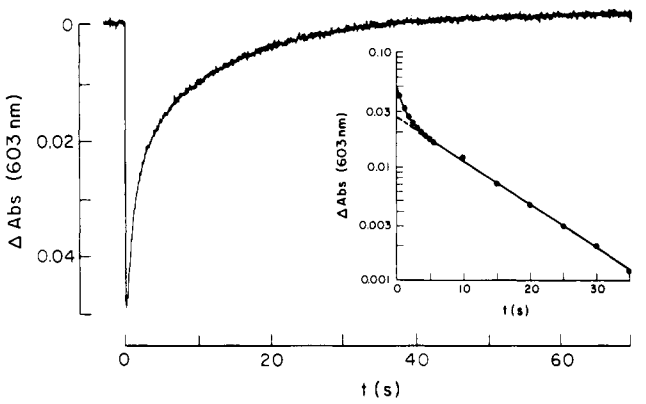

Figure 3. Kinetic trace of $C_{16}MV^{2+}$–DHP reduction by $Co(CN)_5^{3-}$ ion. Conditions: 3.1 μM $C_{16}MV^{2+}$, 0.3 mM $Co(CN)_5^{3-}$, 2 mM DHP in 0.05 M KCN, pH 11.4, 23 °C. Stopped-flow mixing was initiated at $t = 0$. Inset: Logarithmic plots of ΔAbs against time illustrating the biphasic nature of the reaction. The difference between measured ΔAbs and values extrapolated from the linear portion of the curve was also plotted as first order.

Table I. Kinetic Summary[a]

$n(C_nMV^{2+})$	k', M^{-1} s^{-1} [b]	10^4k, M^{-2} s^{-1} [c]	$A_2/(A_2 + A_3)$[d]
6	0.9 ± 0.3	30 ± 17	1.0
8	0.12 ± 0.01	16 ± 4	1.0
10	0.14 ± 0.03	27 ± 6	1.0
14	not seen	7.0 ± 0.4 0.72 ± 0.31	0.76 ± 0.07
16	not seen	3.3 ± 1.6 0.32 ± 0.05	0.53 ± 0.09
18	not seen	1.6 ± 0.2 0.41 ± 0.12	0.75 ± 0.09

[a] Conditions: $\mu = 0.05$ M (KNO_3), 2 mM DHP, 4–6 μM C_nMV^{2+}, 0.05–1.0 mM $Co(CN)_5^{3-}$, 0.01–0.05 M KCN, pH 11.4 at 23 °C. Error limits cited are average deviations from the mean values. [b] $k' = (a/c)/[Co(CN)_5^{3-}][CN^-]$, defined by eq 3–5 as k_1'. [c] $k = (b/c)/[Co(CN)_5^{3-}][CN^-]$, defined by eq 3–5 as $k_1'(k_2[C_nMV^{2+}] + k_3[C_nMV^{2+}]')/k_{-1}'$. [d] Fractional relative amplitude of the fast component of concurrent first-order reactions.

Although it is not explicitly considered in the kinetic analysis, a possible molecular basis for this term is discussed below.

With the longer chain C_nMV^{2+} ions, $n \geq 14$, the reaction rates are several-fold slower under comparable conditions and the zero-order component is lost. Viologen radical ion formation now appears biphasic with both components first order in C_nMV^{2+} concentration (Figure 3). Both terms are first order in $Co(CN)_5^{3-}$ and CN^- concentration within a relatively wide data scatter, which appears typical for C_nMV^{2+}–DHP suspensions.[8] The relative magnitudes of contributions from either pathway and their rate constants are dependent upon the viologen alkyl chain lengths.

Kinetic constants for all of the reactions are listed in Table I. Where examined, rate parameters were wavelength-independent over the visible spectral region and insensitive to variations in C_nMV^{2+}/DHP ratios from 1/500 to 1/125, which is the experimental range spanned in these studies.

Discussion

Electron-Transfer Pathway. Because the Co(III) ions are substitution-inert, product analysis can be used to distinguish between inner- and outer-sphere electron-transfer pathways. For MV^{2+} and C_6MV^{2+}–DHP, $Co(CN)_6^{3-}$ is formed, indicating that electron transfer is outer sphere.[20] The first-order CN^- dependence exhibited for all pathways for all the C_nMV^{2+}–DHP ions supports an outer-sphere assignment for the other ions as well. This result is expected in any event because the dialkylbipyridinium ions possess no nucleophilic sites capable of coordinate bond formation with $Co(CN)_5^{3-}$ ion.

Reaction Mechanisms. A minimal reaction scheme consistent with the rate law is

$$Co(CN)_5^{3-} + CN^- \underset{k_{-1}'}{\overset{k_1'}{\rightleftharpoons}} (Co(CN)_6^{4-})_i \quad (3)$$

$$(Co(CN)_6^{4-})_i + C_nMV^{2+}\text{–DHP} \xrightarrow{k_2} Co(CN)_6^{3-} + C_nMV^{+}\text{–DHP} \quad (4)$$

$$(Co(CN)_6^{4-})_i + C_nMV^{2+}\text{–DHP}' \xrightarrow{k_3} Co(CN)_6^{3-} + C_nMV^{+}\text{–DHP} \quad (5)$$

where the primes on k_1' and k_{-1}' are taken to indicate that these constants are for formation and ligand dissociation of interfacial $Co(CN)_6^{4-}$, which, by virtue of proximity to a highly negatively charged surface, must be at a lower concentration than in bulk solution, and the prime on C_nMV^{2+}–DHP′ indicates a binding environment distinct from that of C_nMV^{2+}–DHP. Applying the steady-state approximation to $(Co(CN)_6^{4-})_i$, one obtains[21]

$$\frac{d[C_nMV^+]}{dt} = \frac{k_1'\{k_2[C_nMV^{2+}] + k_3[C_nMV^{2+}]'\}}{k_{-1}' + k_2[C_nMV^{2+}] + k_3[C_nMV^{2+}]'}[Co(CN)_5^{3-}][CN^-] \quad (6)$$

For the short-chain viologens ($n \leq 10$), either $k_2 = k_3$ or, more likely, there exists only a single binding domain on the vesicles so that $[C_nMV^{2+}]' \simeq 0$. Equation 6 then reduces to the form of eq 1, where $a/b = (k_1'k_2/k_{-1}')[Co(CN)_5^{3-}][CN^-]$ and $a/c = k_1'[Co(CN)_5^{3-}][CN^-]$. For the longer chain analogues ($n \geq 14$), $k_{-1}' > k_2[C_nMV^{2+}]$ and $k_3[C_nMV^{2+}]'$ so that the approximate solution to eq 6

$$d[C_nMV^+]/dt = (k_1'/k_{-1}')\{k_2[C_nMV^{2+}] + k_3[C_nMV^{2+}]'\}[Co(CN)_5^{3-}][CN^-] \quad (7)$$

is observed.

The second-order constant k_1' is the interfacial CN^- ligand association rate constant, which should be dependent upon the identity of bound C_nMV^{2+} ions only to the extent that the latter modifies the DHP vesicle surface charge. At the very light viologen loadings used in these experiments, this perturbational influence should be minimal. Consequently, k_1' should be nearly invariant through the series of C_nMV^{2+}–DHP particles. This condition is met for C_8MV^{2+} and $C_{10}MV^{2+}$ and is consistent with results for the long-chain viologens (Table I). However, k_1' for C_6MV^{2+} appears unusually high. As mentioned in Results, there is evidence from the rate curves for contribution from an additional pathway when $[Co(CN)_5^{3-}][CN^-]$ is low. This pathway might involve reaction of C_6MV^{2+} that is not vesicle-bound and could account for the apparent increase in k_1' in this reaction. Inclusion of the following steps in the rate law for short-chain viologens

$$C_nMV^{2+}\text{–DHP} \overset{k_4}{\rightleftharpoons} (C_nMV^{2+})_f + \text{DHP} \quad (8)$$

$$(C_nMV^{2+})_f + Co(CN)_6^{4-} \rightarrow C_nMV^+ + Co(CN)_6^{3-} \quad (9)$$

yields[21]

$$\frac{d[C_nMV^+]}{dt} = \left\{\frac{k_1'k_2[Co(CN)_5^{3-}][CN^-]}{k_{-1}' + k_2[C_nMV^{2+}]} + k_4\right\}[C_nMV^{2+}] \quad (10)$$

when release of C_6MV^{2+} from the vesicle surface is rate-limiting for this pathway. Because hydrophobic interactions contribute significantly to the binding forces of single-chain amphiphiles to vesicles, k_4 should decrease with increasing alkyl chain length for the C_nMV^{2+} ions. Similarly, from the form of the rate law, the relative contribution of k_4 will diminish as $[Co(CN)_5^{3-}][CN^-]$ increases. Both effects are observed, supporting this interpretation.

(20) Candlin, J. P.; Halpern, J.; Nakamura, S. *J. Am. Chem. Soc.* **1963**, *85*, 2517–2518.

(21) Since C_nMV^{2+} ions are essentially completely DHP bound, we write $[C_nMV^{2+}]$ to indicate $[C_nMV^{2+}$–DHP], etc.

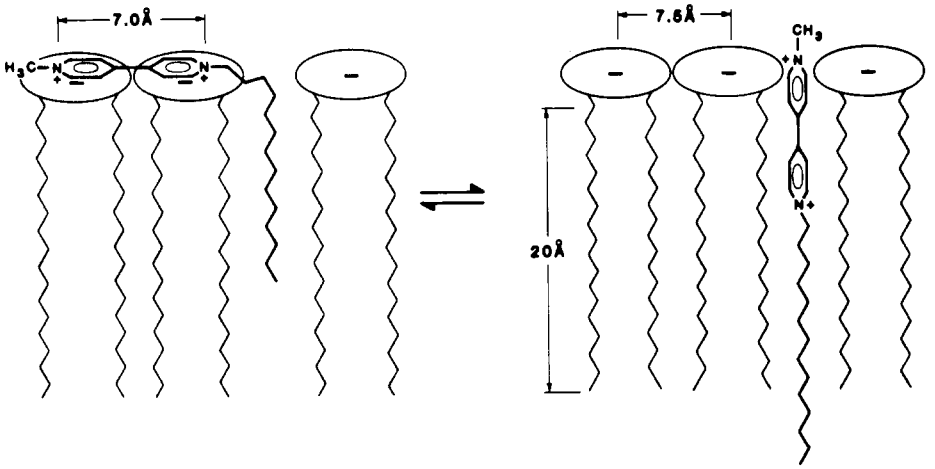

Figure 4. Hypothetical two-state model for $C_{14}MV^{2+}$ binding in the lateral plane of DHP vesicles.

Reduction following release of DHP-bound C_6MV^{2+} has also been inferred from rate measurements in reaction with dithionite ion.[8]

Interpretation of Biphasic Reduction of C_nMV^{2+}–DHP, $n > 14$. For the long-chain viologens, two distinct binding domains that do not interconvert on the kinetic time scale are suggested from the rate law (eq 7). Because the concentration of viologen free in solution is negligible, the biphasic behavior cannot be attributed simply to free vs. bound C_nMV^{2+} ions. Similarly, there is no evidence of particle heterogeneity. Light-scattering results indicate a unimodal distribution of vesicle sizes,[10] and the presence of C_nMV^{2+} micelles, which might be difficult to detect by this method, is precluded because the analytical concentrations of viologens used are far below their critical micelle concentrations.[22] Binding inhomogeneities, which might arise as artifacts of the loading process, can be excluded because photochemical kinetics experiments have shown that asymmetrically loaded C_nMV^{2+}–DHP vesicles reach their equilibrium distribution within less than 2 min.[9] Distribution between surface-aggregated and monomeric forms also appears unlikely in these highly diluted systems. No evidence for surface association exists in the optical spectrum of the product C_nMV^+ radical ions, which is quite sensitive to aggregation,[17] and a detailed investigation of the ionic strength dependence of similar biphasic reactions of SO_2^- ion with C_nMV^{2+}–DHP vesicles gave no indication of differences in the reactant electrostatic charge,[8] which would be expected if viologens were aggregated at one of the reaction sites.

One infers by default the simultaneous existence of two distinct binding sites for monomeric long-chain viologens within a single vesicle. These separate sites cannot represent the opposite vesicle interfaces because the rate law is inappropriate for either of the steps being transmembrane redox.[6] Rather, in addition to surface adsorption, the long-chain viologens might possibly intercalate into the bilayer structure, as suggested in Figure 4. In the figure, ellipses are used to represent the phosphate head groups, which can assume O^- to O^- separation distances from about 5.3 to 7.6 Å, depending upon the packing geometry.[23] Since the bipyridinium N–N distance[24] is 7.0 Å, simultaneous ion pairing to two neighboring head groups is readily achieved. The distribution may exist for longer chains because electrostatic forces lost upon intercalation are compensated by increased hydrophobic interactions between the alkyl chain of viologen and surfactant. Furthermore, reactivity of the intercalated form may be less (Table I) simply because accessibility to aqueous reductants is limited. Similar models have recently been advanced to account for the photophysical behavior of structurally similar monoalkylstilbenes.[2] Some evidence consistent with the model is that DHP vesicle sizes appear to increase upon addition of long-chain viologens, as would occur with incorporation into the bilayer, but no such swelling is evident upon adding short-chain analogues.[10] The kinetics indicate that the activation barrier for conversion between the forms is substantial. This point is not addressed by the simple model presented but implies that extensive rearrangement of the bilayer structure also occurs.

Other Mechanistic Aspects. Rates of photochemical reduction of C_nMV^{2+}–DHP vesicles by triplet (5,10,15,20-tetrakis(4-sulfonatophenyl)porphinato)zinc(II) ($ZnTPPS^{4-}$) ion are consistent with an encounter-controlled process[9] whereas chemical reduction by SO_2^- ion appears to require collisional activation.[8] Comparable analysis of this reaction is not possible because thermodynamic parameters for $Co(CN)_6^{4-}$ formation are unknown. However, a lower limit for the interfacial CN^- ligand association constant (eq 3) can be estimated from the rate data. From phenomenological theory,[25] $k_d = k_o[\gamma/(e^\gamma - 1)]$, $\gamma = z_A z_B e^2/4\pi\epsilon rkT$, where k_d, the diffusion-limited rate constant, is defined by

$$d[C_nMV^+]/dt = k_d[Co(CN)_6^{4-}][C_nMV^{2+}] \qquad (11)$$

Under the experimental conditions,[8,9] $k_o \simeq 10^{11}$ M^{-1} s^{-1}, $z_A z_B$ = 30–40, and $\epsilon r \simeq 100$, giving $k_d \simeq (0.3–20) \times 10^5$ M^{-1} s^{-1}. From comparison of eq 7 and 11, $K'k_d \geq k_1'k_2/k_{-1}'$, where $K' = [Co(CN)_6^{4-}]/[Co(CN)_5^{3-}][CN^-]$, and using $k = k_1'k_2/k_{-1}' = 3 \times 10^5$ M^{-1} s^{-1} from Table I, we obtain $K' \geq 0.1$–10 M^{-1}. This range of values for the interfacial ligand association constant exceeds by 10^2-fold a similar estimate made for homogeneous solution.[20] Although there is considerable margin for error in the parameters assumed for the calculation, the results do suggest that the presence of the interface does not drastically alter the ligand association–dissociation equilibrium.

More dramatic effects are seen in comparing ligand association rates. Dissocation of CN^- from $Co(CN)_6^{4-}$ to give the square-pyramidal $Co(CN)_5^{3-}$ ion[26] should occur with minimal reorganization of the cobalt primary coordination sphere. Taking $k_{-1} \simeq 10^9$ s^{-1} as a reasonable estimate for the dissociation rate constant and the estimated magnitude of the equilibrium constant from above, it follows that $k_1 \simeq 10^5$–10^8 M^{-1} s^{-1}. From the experimental data (Table I), the measured interfacial association rate constant is only $k_1' \simeq 0.1$ M^{-1} s^{-1}, which reflects the virtual depletion of reactant anions from the diffuse double layer as a consequence of electrostatic repulsion by the vesicle surface.[27]

The most significant finding of notion work is that it provides independent support for the notion that two types of binding sites for long-chain viologens exist in DHP vesicles. The kinetic be-

(22) Brugger, P.-A.; Infelta, P. P.; Braun, A. M.; Grätzel, M. *J. Am. Chem. Soc.* **1981**, *103*, 320–326.
(23) Hunt, E. C. *J. Colloid Interface Sci.* **1969**, *29*, 105–115.
(24) Summers, L. A. *The Bipyridinium Herbicides*; Academic: New York, 1980; p 96.
(25) Debye, P. *Trans. Electrochem. Soc.* **1942**, *82*, 265–272.
(26) Tsay, F.-D.; Gray, H. B.; Danon, J. *J. Chem. Phys.* **1971**, *54*, 3760–3769. Brown, L. D.; Raymond, K. N. *Inorg. Chem.* **1975**, *14*, 2590–2594.
(27) For this reason, interfacial dynamics should be strongly dependent upon the surface potential of the vesicle. In these studies, care was taken to maintain the C_nMV^{2+}/DHP ratio nearly constant to minimize variations in surface potentials that might otherwise compromise rate comparisons.

havior of this system is analogous to that for C_nMV^{2+}-DHP reduction by SO_2^- ion.[8] In the latter system, circumstantial evidence was obtained suggesting that transmembrane redox is carried only by electron exchange between the "buried" viologens.[28] Exposition of the molecular organization at the reactive sites is therefore crucial to developing an understanding of transmembrane redox processes.[6] To this end, we are currently studying viologen-DHP interactions by a variety of structural techniques.

(28) Attempts to study transmembrane redox in this system were obviated because the C_nMV^{2+} ions underwent extensive degradation under the conditions required for DHP vesicle formation, i.e., high temperature and alkaline media. It was not possible, therefore, to prepare vesicles with C_nMV^{2+} bound at both interfaces.

Acknowledgment. Financial support for this research was provided by a grant from the Division of Chemical Sciences, U.S. Department of Energy (Grant No. DE-AC-06-83ER13111). The digital oscilloscope used in the fast-kinetics studies was obtained through a grant (Grant No. 8522) from the Medical Research Foundation of Oregon. The authors are deeply grateful to these agencies for their program support. It is also a pleasure to acknowledge stimulating discussions with Dr. James Espenson concerning reaction mechanisms, the assistance of Eberhardt Kuhn in analyzing some of the data, and the interest of Dr. William C. Barrette, Jr., who first suggested this study.

Contribution from the Department of Chemistry, Willard Hall, Kansas State University, Manhattan, Kansas 66506

Cleavage Reactions of Bridged Structures. Asymmetric Cleavage of Diborane: A Case of Counterintuitive Orbital Control of Reaction Products

Keith F. Purcell* and David D. Devore

Received April 23, 1986

As prototypes of inorganic bridge structure cleavage reactions by Lewis base attack, those of diborane are of two types: symmetric (2 LBH_3 as product) and asymmetric ($L_2BH_2^+BH_4^-$ as product). The known structure $(LBH_2)H(BH_3)$ likely appears as an intermediate in these cleavage reactions and serves as a model for the microstudy of the cleavage. This article addresses the question of orbital steering of the second ligand-interchange step of L for H(bridge) at boron, the step that consummates the cleavage reactions. We conclude that there is electronic steering favoring geminal (asymmetric) entry of the second Lewis base molecule. Generalization of our findings for this molecule clarifies the roles of the electronegativity and orbital type of the bridge atom and of the long-range bridgefoot orbital interference energies in the general phenomenon of cleavage of inorganic bridge structures, of which $(LBH_2)H(BH_3)$ is but one example.

Introduction

Inorganic bridged structures are pervasive, and bridge-cleavage reactions are of fundamental importance to electron-transfer, mixed-valence and polynuclear catalysis reactions. While there have been many investigations of bridge electronic structures, much less attention has been given to understanding how such bridges are cleaved by Lewis acids and bases. The works of Shore, of Parry, and of Jolly on the cleavage of diborane by Lewis bases present an interesting case, with cleavage leading to either of two types of products: simple borane adducts result from symmetric cleavage (eq 1), and salts are produced from unsymmetric cleavage (eq 2).[1] It is to be presumed that these cleavage reactions proceed

$$B_2H_6 + 2L \rightarrow 2LBH_3 \quad (1)$$

$$B_2H_6 + 2L \rightarrow L_2BH_2^+BH_4^- \quad (2)$$

through a common "half-opened" intermediate, LB_2H_6, resulting from an interchange attack by a single L molecule upon B_2H_6. In fact, the "half-opened" structures have been prepared independently through reactions like (3).[2] The cleavage of **1** is geminal

$$2LBH_3 + B_2H_6 \rightarrow \underset{\mathbf{1}}{2(LBH_2)H(BH_3)} \quad (3)$$

(B_g) or vicinal (B_v) to the substituted boron and may proceed by a B–H_b dissociative reaction step or by a ligand-interchange step of L for H_b.

The experimental product distributions observed for sterically hindered and unhindered donors suggest that, in the absence of steric factors, asymmetric cleavage is favored (reaction 2). To account for this observation, one can propose either dissociative cleavage of **1** at B_g–H_b or ligand interchange at B_g involving L–B_g bond-forming and B_g–H_b bond-breaking components. At first glance, the experimental result might be attributed simply to an interchange step with classical electrostatic forces directing L to the more electrophilic boron atom, B_g. The same forces operating within **1** would, however, favor stronger B_g–H_b than H_b–B_v bonding, favoring reaction 1 in either a dissociative or interchange step. Even more troublesome to us is the naiveté of such classical arguments in ignoring the orbital interference requirements of interchange and dissociative reaction steps. To complicate matters, the steric congestion differential for B_g and B_v should direct L to B_v, generally.

These questions merit an analysis of the *electronic* control by intermediate **1** of the site of entry of L in the second interchange step.[4,5] The primary conclusion of this report is that there is electronic steering of the second donor to B_g in **1**, whether the cleavage is dissociative or associative, and that this geminal regiospecificity is soundly based in the orbital topology of the three-center bridge unit. Furthermore, we have been able to establish the requirements for chemical tuning of this topology to select geminal or vicinal attack.

Calculational Methods

Standard INDO calculations[6] were performed for the "half-opened" intermediate $(H_3NBH_2)H(BH_3)$ using tetrahedral angles and representative bond distances; Figure 1 presents a representation of the structure of the "half-open" intermediate in the presence of an approaching NH_3 molecule.

The INDO molecular orbital functions were renormalized with overlap integrals included in order to obtain more realistic contour maps of orbital amplitudes.[7] The graphical presentations given here result from calcu-

(1) McAchran, G. E.; Shore, S. G. *Inorg. Chem.* **1965**, *4*, 125. Shore, S. G.; Hickam, C. W.; Cowles, D. *J. Am. Chem. Soc.* **1965**, *87*, 2755. Rudolph, R. W.; Parry, R. W.; Farran, C. F. *Inorg. Chem.* **1966**, *5*, 723. Schultz, D. R.; Parry, R. W. *J. Am. Chem. Soc.* **1958**, *80*, 4. Shore, S. G. *Ibid.* **1958**, *80*, 8. Beachley, O. T. *Inorg. Chem.* **1965**, *4*, 1823. Finn, P.; Jolly, W. L. *Ibid.* **1972**, *11*, 1941.

(2) Shore, S. G.; Hall, C. L. *J. Am. Chem. Soc.* **1966**, *88*, 5346. Shore, S. G.; Hall, C. L. *Ibid.* **1967**, *89*, 3947.

(3) Purcell, K. F.; Kotz, J. C. *Inorganic Chemistry*; W. B. Saunders: Philadelphia, PA, 1977: (a) p 400; (b) p 109; (c) pp 657, 674.

(4) Young, D. E.; Shore, S. G. *J. Am. Chem. Soc.* **1969**, *91*, 3497.

(5) Moews, P. C., Jr.; Parry, R. W. *Inorg. Chem.* **1966**, *5*, 1552.

(6) Pople, J. A.; Beveridge, D. L. *Approximate Molecular Orbital Theory*; McGraw-Hill: New York, 1970. A locally modified version of the standard INDO program was used.

(7) Offenhartz, P. O. *Atomic and Molecular Orbital Theory*; McGraw-Hill: New York, 1970; Appendix 2.

0020-1669/87/1326-0043$01.50/0